

The impact of the London Olympic Parkland on the urban heat island

Ian Hamilton^{a*}, Jenny Stocker^b, Stephen Evans^c, Michael Davies^d and David Carruthers^b

^aUCL Energy Institute, The Bartlett, University College London, 14 Upper Woburn Place, London WC1H 0NN, UK; ^bCambridge Environmental Research Consultants Ltd., 3 King's Parade, Cambridge CB2 1SJ, UK; ^cCentre for Advanced Spatial Analysis, The Bartlett, University College London, 1-19 Torrington Place, London WC1E 6BT, UK; ^dBartlett School of Graduate Studies, The Bartlett, University College London, 14 Upper Woburn Place, London WC1H 0NN, UK

(Received 6 January 2012; final version received 27 March 2013)

The London Olympic Parkland represents a substantial area of redevelopment with the potential to significantly modify urban temperatures. This paper illustrates a neighbourhood-scale model of the type that can be used to analyse the impact of large developments on the urban heat island, using the London Olympic Parkland as an example. Using the *Atmospheric Dispersion Modelling System Temperature and Humidity* model, the impact of the urban surfaces for the Parkland area (~16 km²) is modelled at a 400 m² grid resolution for the pre-Olympic, Olympic and Legacy periods. Temperature perturbations from upwind values are simulated for the periods to estimate the contribution the Parkland has on local air temperatures. The results illustrate the impact that large impermeable features such as the concourse might have on increased air temperatures during Olympic period design conditions. In comparison, a Legacy scenario shows temperature reductions from the pre-Olympic period due to an increase in vegetation coverage.

Keywords: urban heat island; air temperature; urban form; master plan; mitigation; atmospheric modelling

1. Introduction

The Olympic Parkland development represents one of the largest land-use changes to be experienced within London over the past 40 years, with approximately 12.5 km² of land being reformed within greater London. The scale of the alteration that the Olympic site will have on London's urban fabric has the potential to affect the urban climate, in particular the impact that the redevelopment will have on the local temperature experienced in and around the site, and also the potential influence on London's urban heat island (UHI). The primary consideration of this paper is to highlight the potential of a neighbourhood-scale urban-climate model to investigate the impact that designs at this scale could have on urban temperatures. We consider three designs of the London Olympic Parkland as follows: the Olympic period (approximately 2012/2013, after the Olympic event) and the Olympic Legacy (approximately 2030), which are compared to the pre-Olympic conditions (approximately 2006). The proposed designs for the Legacy period are still largely in a draft form and are likely to change prior to their completion. The neighbourhood model is described and a sensitivity study is undertaken to show how changes to the model inputs provide results within expected ranges. We also discuss the limitations of the assumptions made for the designs and the input modelling parameters.

1.1. The UHI

Here, we provide a brief description of the UHI—references to more exhaustive treatments are noted in the text. In essence, the UHI is the difference in temperature between the urban or built environment and the surrounding rural zone (Oke 1973, 1987; Taha 1997; Arnfield 2003). The UHI represents the impact that urban features, such as hard surfaces and lack of vegetation, have on the rural environment, causing a difference in temperature and humidity. Oke (1995) has described this change in the urban climate as a visible product of local scale man-made climate change.

The UHI's formation is broadly determined by the ability of the urban fabric and materials to capture, store and release energy (known as energy exchange) largely from incoming solar radiation, thus affecting the surface energy balance. The urban morphology influences heat release, convection and advection in the urban boundary layer, which affect the surface momentum energy exchange by altering long and short-wave radiation exchange and the turbulence of the roughness sublayer. Urban land use and, in particular, the location, prevalence and size of green space contributing to evaporation and evapotranspiration throughout the urban fabric also affect the storage parameters of the energy exchange by reducing the amount of incoming solar radiation absorbed by the surface as well

*Corresponding author. Email: i.hamilton@ucl.ac.uk

as the latent and sensible heat flux. Further, sources of anthropogenic heat emission, for example, vehicles, buildings and industry, add to the heat emission and affect the overall heat balance (Taha 1997; Ichinose, Shimodozono, and Hanaki 1999; Offerle, Grimmond, and Fortuniak 2005; Hamilton et al. 2009; Sailor 2010) and have been shown to increase the temperature due to the UHI, i.e. the UHI increment (UHII) by 1–2°C (Ichinose, Shimodozono, and Hanaki 1999; Bohnenstengel et al. 2011). This source of additional energy release is added as a positive value to the surface energy balance. The formation and presence of the heat island throughout a city are thus influenced by the composition of the urban fabric and the activities within. The formation of the UHI is also influenced by the land use and topography of the adjacent ‘non-urban’ zones. Sprawling urban forms or nearby conurbations can increase the build-up of heat in the lower boundary layer, limiting the ability for wind and turbulence to dissipate heat built up in the core of the urban zone (Bohnenstengel et al. 2011). For a more exhaustive review of the UHI development we recommend Arnfield (2003) along with the other authors cited above.

Within the urban environment, the UHI will affect infrastructure and air quality (for instance, ozone levels) as well the health and thermal comfort of the population (Ojima 1990; Knowlton et al. 2008; McMichael et al. 2008). The degree of impact is highly dependent on a number of factors, including: a buildings’ ability to resist overheating; the availability and amount of green space; the penetration of air conditioning systems; and the type of road surfacing and its ability to maintain structural integrity. During heat wave periods, the UHII, i.e. the additional input of heat resulting from the heat island, can further exacerbate these impacts. Positive effects of the UHI include reducing heat demand in buildings in heating-dominant climates.

Strategies that aim at mitigating the UHI include the following: increasing the albedo or reflectivity of the urban surfaces to reduce the amount of solar energy captured and stored; adding more green spaces to act as heat sinks and increase evapotranspiration and shading; and reducing direct sensible heat emissions from buildings and vehicles (Environmental Protection Agency 2009).

1.1.1. London’s UHI

London’s UHI is well described (for example, Howard 1818; Watkins et al. 2002; Kolokotroni and Giridharan 2008; Bohnenstengel et al. 2011; Mavrogianni et al. 2011), and the nocturnal summertime UHII has been shown to be approximately 2°C (Kolokotroni and Giridharan 2008). During periods of extreme weather, for example, the 2003 heat wave, parts of central London were up to 10°C warmer than the surrounding rural zone (GLA 2010). The approximate epicentre of London’s UHI is located to the east of British Museum, over London’s financial district, an area characterized by dense urban form and little green space.

In London, the Greater London Authority (GLA) has identified the UHI as an important issue with respect to summertime overheating and climate change mitigation and adaptation. In their planning documents, the GLA have included specific policies that require new development to address the effect they have on the UHI, there are also specific policies that attempt to target local climate change through UHI mitigation efforts, such as increasing urban street trees (GLA 2006, 2009, 2010)

Surface features, such as the urban fraction, i.e. the area of hard surface, are shown to correlate well with UHI intensity (Bohnenstengel et al. 2011). Anthropogenic heat emission sources in London have been shown to be a sizeable component of the total heat flux, as compared to the incoming solar radiation, with emissions in dense urban areas being the highest (Hamilton et al. 2009; Iamarino, Beevers, and Grimmond 2012).

1.1.2. Influencing features of London’s UHI

The land use of London consists of predominantly permeable surfaces. Approximately 65% of the land surface area is domestic gardens, green spaces and parks or bodies of water, 14% is roads, rail or paths, 14% buildings and the remaining 7% ‘other’ (Office of National Statistics 2005). Defining the ‘urban fraction’ of an area to be the proportion of impermeable surfaces, on average, London’s urban fraction is approximately 0.35; however, in areas of high building density, this fraction can be greater than 0.5.

The annual average anthropogenic heat emission across London is approximately 9 W/m², but can be up to 550 W/m² during a winter’s day in the core of London or 220 W/m² during a summer’s day (Hamilton et al. 2009).

In developing strategies that alter London’s urban fabric, such as the London Olympic Parkland, the urban fraction and contribution of anthropogenic-related heat emissions play an important role in London’s overall UHI and changes to neighbourhood level temperatures.

1.2. London Olympic Parkland

The total area of the Olympic development site is approximately 12.5 km², located between the borders of five of London’s boroughs, along the Lea River Valley. Here, we characterize the site into three periods: pre-Olympics (circa 2006), Olympic period (circa 2012/2013) and Olympic Legacy (circa 2030) (see Figure 3). Table 1 summarizes the Olympic Parkland development site features during these three periods.

The pre-Olympic period has approximately 34% permeable area (green space, gardens and water) and 38% impermeable urban area (i.e. buildings, roads, paths and rail). The Olympic period sees the removal of industrial warehouses and conversion of land along the river and the addition of Olympic venues and green space along with a large concourse and ‘back of house’ area throughout the

Table 1. Olympic Parkland development site features as a percentage of the total development area.

Site feature	Pre-Olympics (2006) (%)	Olympic period (2012) ^a (%)	Olympic Legacy (2030) ^a (%)
Water	4	5	5
Domestic buildings	0	1	1
Non-domestic buildings	3	5	4
Roads	3	12	4
Paths	0	0	0
Rail	31	12	13
Green space	30	33	43
Domestic gardens	0	0	0
Other	28	32	30
Total	100	100	100

^aEstimates of land use are indicative only and do not reflect the final design.

site; at this time the impermeable surfaces reduce slightly to 34% (this includes the addition of the concourse, approximately 4% of the ‘Other’ category). Note that the special requirements for pedestrian and goods and services during the Olympic period mean that hard surfacing is present throughout the parkland. The Legacy period proposes the development of a new urban district surrounding the Queen Elizabeth Olympic Park, which increases the overall permeable fraction to 48%, approximately a 13% increase in green space compared to the pre-Olympic period, along with an increase in the area of buildings.

1.3. Modelling London’s UHI

Under the Engineering and Physical Sciences Research Council-funded LUCID project, a series of scaled climate models were developed to investigate London’s UHI (i.e. city, neighbourhood and street), see Mavrogianni et al. (2011) for a description of LUCID project and models, along with Bohnenstengel et al. (2011), Porson et al. (2009) and White and Holmes (2009). Here, we illustrate the potential of a neighbourhood-scale temperature model, the *Atmospheric Dispersion Modelling System (ADMS) Temperature and Humidity* model, to help understand the possible impact of a development such as the proposed Olympic site on temperatures at a local level, by using it to predict the perturbations of air temperature at the Olympic development site for the three periods of interest (i.e. pre-Olympics, Olympic period and Olympic Legacy).

2. Methodology

2.1. ADMS Temperature and Humidity land-use model

The neighbourhood-scale *ADMS Temperature and Humidity* land-use model (CERC 2010) uses local estimates of a

range of surface properties and the building density to calculate local perturbations of temperature and humidity to upwind meteorological (boundary) conditions predicted by the London Unified Model (LondUM). LondUM is a time-dependent grid-based numerical model designed to take account of the surface characteristics of an urban area at 1 km resolution, the model is typically used for domains in the range 1–50 km² (Bohnenstengel et al. 2011). The *ADMS Temperature and Humidity* model is a deterministic model based on the ADMS (Carruthers et al. 1994) and brings together previously published models for perturbations to flow, temperature and humidity into one modelling framework. The key components of the model are the ADMS meteorological pre-processing module (Thomson 2000), which has been adapted to link with outputs from LondUM, and the ADMS module for flow over complex terrain (FLOWSTAR; Carruthers, Hunt, and Weng 1988), which has been modified to calculate perturbations of temperature (ϑ_i) and humidity (q_i) to the upwind flow over surfaces of varying characteristics, based on the work presented by Carruthers and Weng (1992). ϑ_i and q_i are calculated from the governing conservation equations using the uncoupled variables a and b in Fourier space, which are related to ϑ_i and q_i over the complex surface by

$$\vartheta_i = \frac{a + b}{pC_p(S + 1)}$$

and

$$q_i = \frac{Sa - b}{p\lambda(S + 1)},$$

where, $S = (\lambda/c_p)dq_3/dT$ is evaluated at $T = T_0$, q_s is the saturated specific humidity at temperature T , C_p is the specific heat capacity of air, p is the density of air and λ is the latent heat for the vaporization of water, and the Fourier transformation of variable a is defined as

$$\tilde{a} = (k_1, k_2, z) = \int_{-\infty}^{\infty} \int_{-\infty}^{\infty} a(x, y, z) e^{-ik_1x - ik_2y} dx dy.$$

We take the inverse Fourier transforms of following Carruthers and Weng (1992) and calculate the perturbations in potential temperature (ϑ_i) and specific humidity (q_i).

The governing equations are expressed in terms of parameters that account for perturbations to the surface resistance to evaporation parameter and the normalized surface value of the net heating perturbation. Here, the latter parameter is calculated as the difference between the net radiation and ground heat flux perturbation parameters. The development of the FLOWSTAR module to include the effects of a shear stress perturbation due to changes in the local surface roughness derives directly from the analysis of Raupach et al. (1992). Although the neighbourhood-scale model described above is able to predict both temperature and humidity variations, in this work only the temperature predictions are discussed.

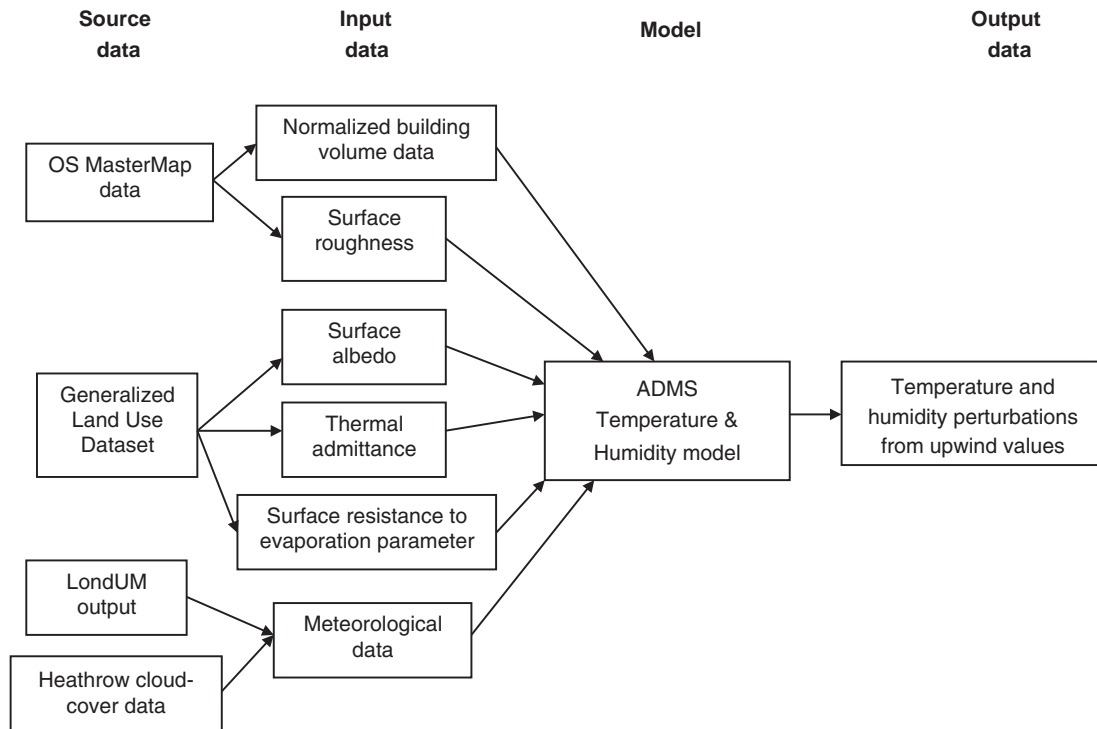


Figure 1. ADMS Temperature and Humidity model set-up.

Hamilton et al. (2009) present results showing the relationship between the normalized building volume (NV) parameter and the incoming short-wave radiation, for a surface albedo of 0.2. This work is extended to cover a range of surface albedos. It has been possible to derive a prediction for the spatial variation of incoming short-wave radiation with change in surface albedo and NV. The spatial variation of the ground heat flux perturbations are calculated using the local estimates of the thermal admittance and surface resistance to evaporation parameter. The ADMS meteorological pre-processor (Thomson 2000) calculates hourly predictions for the upwind temperature and humidity boundary-layer profiles from basic meteorological parameters. However, for the current study, the module has been adapted to use estimates of the upwind surface sensible, latent and ground heat flux parameters output from the LondUM (Bohnenstengel et al. 2011) to predict more detailed upwind boundary-layer profiles. Figure 1 shows the *ADMS Temperature and Humidity* model relationship.

Uncertainty within the model outputs will be associated with the input upwind temperature and heat flux value parameters from LondUM, the model dynamics (i.e. the perturbation to the mean flow and turbulence due to the surface roughness and the transport and diffusion of sensible and latent heat near the surface) and the specification of land-use changes and their relations to the model parameters used to represent the surface (that is, albedo, thermal admittance, surface resistance to evaporation and NV). LondUM has been shown to simulate temperatures within an accuracy

range of 1–2 K (Bohnenstengel et al. 2011). The application of this perturbation model to sensitivity studies demonstrates that the sign of the perturbations due to the different land surface variations is generally correct – described further below and in the appendix. For instance, increasing surface wetness reduces the temperature, increasing albedo reduces the temperature during daytime, and increasing thermal admittance reduces the temperature in the early morning but causes an increase in the late afternoon and at night, as stored heat is re-released to the atmosphere.

2.1.1. Anthropogenic heat

While the *ADMS Temperature and Humidity* model described above is able to account for local perturbations in temperature and humidity due to land-use changes, it does not account for anthropogenic heat. The most significant sources of anthropogenic heat in London within an urban area are buildings and road transport (Davies et al. 2008). One approach to modelling the spatial variation of heat generated from these sources is to define a heat concentration parameter, which is analogous to a source of air pollutants, such as NO_x or particulates. In this work, we assume that the dispersion of heat occurs in much the same way as air pollutants and we use a Gaussian plume dispersion model (CERC 2011) to predict the spatial distribution of anthropogenic heat from buildings and roads, either on an hourly basis, or in terms of a long-term average.

2.1.2. ADMS Temperature and Humidity model testing

A description of the sensitivity analyses performed and results are presented in the appendix. The results of the sensitivity study show the perturbations to the upwind profile of temperature and humidity predicted by the model performs as expected with respect to the sign of the temperature perturbation predicted for bulk changes in input parameters. With regard to model uncertainty, it should be noted that the morphological features of the surface are smoothed for the model formulation and therefore the model does not resolve temperature perturbations for the street scale. Also, the model predicts hourly average temperature perturbations, using hourly average meteorology, but in reality there are fluctuations in meteorology over short time and spatial scales; the model does not resolve these.

A validation of the neighbourhood *ADMS Temperature and Humidity* model is fully described in Stocker et al. (forthcoming), which provides a comparison of *ADMS Temperature and Humidity* model outputs and several monitored sites around London. The work compares the model results with measured temperatures for a fixed point in space over a selected period. The comparison results show that the *ADMS Temperature and Humidity* model is able to predict plausible temperature and humidity changes that occur due to changes in land use and anthropogenic emissions. In addition, the input upwind meteorological parameters (i.e. upwind temperature and heat flux value) are drawn from LondUM, which has undergone a validation testing process (Grimmond et al. 2010, 2011). The LondUM acts as a baseline on which the *ADMS Temperature and Humidity* model perturbs the upwind temperatures due to surface and anthropogenic parameters.

Although the testing in the appendix provides some confidence in the use of the model, the results presented here should be considered as indicative and are intended, in large

part, to simply illustrate the potential value of the use of such tools in modelling temperature at a local scale. We should note that the *ADMS Temperature and Humidity* model was used during the London Olympics to provide daily forecasts of temperatures (CERC 2012).

2.2. ADMS Temperature and Humidity model inputs

The *ADMS Temperature and Humidity* model requires estimates of the spatial variation of surface properties within the model domain, specifically: albedo, surface resistance to evaporation parameter, thermal admittance, surface roughness length and NV. In order to apply the model to real-world scenarios, it is necessary to obtain estimates of these parameters in terms of land-use data (to calculate albedo, surface resistance to evaporation parameter and thermal admittance parameter) and site morphology (to calculate surface roughness length and NV).

For this particular study, where different development scenarios are of interest, information from various planning documents has been used to make estimates of land-use changes and anthropogenic heat from buildings. Data associated with the change in road transport due to the development were not available, although this is not seen as a major issue, as the anthropogenic heat from transport is modest compared to building-related emissions, i.e. in London the annual average transport heat flux is approximately 2.5 W/m^2 compared to 13.4 W/m^2 for buildings (Davies et al. 2008).

Figure 2 shows the development area covered by the planning data on which the Olympic development land use, morphology and anthropogenic heat input files is based. The hashed area is the nested region for which model results are presented; beyond this area is a 500 m buffer in which model results are considered to be less accurate due to the edge effect and therefore not used in the analysis.

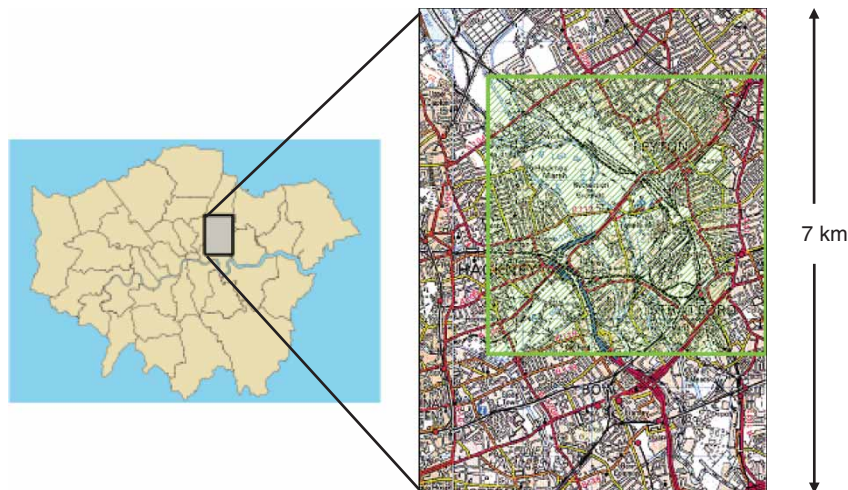


Figure 2. Olympic development site.

Table 2. Summary of parameters associated with the generalized land-use database categories, with an additional entry for reed beds.

GLUD code	Land-use description	Associated parameter values ^a		
		Albedo (-)	Thermal admittance (J/(K m ² s ^{1/2}))	Surface resistance to evaporation parameter (s/m)
0	Unclassified	0.05	1205	200
1	Water	0.8	1545	0
2	Domestic buildings	0.12	1505	200
3	Non-domestic buildings	0.12	1505	200
4	Roads	0.08	1205	200
5	Paths	0.08	1096	200
6	Rail	0.08	1150	200
7	Green space	0.157	600	100
8	Domestic gardens	0.19	600	60
9	Other (mainly hardstanding)	0.05	1205	200
n/a	Reed beds	0.14	1420	100

^aData drawn from Oke (1987) and Stull (1988).

2.2.1. Land use

For the pre-Olympic base case (scenario A), the Generalised Land Use Database (2006) has been utilized. Estimates of the albedo, thermal admittance and surface resistance to evaporation parameter have been made by creating a correspondence between the aforementioned parameters and each of the 10 land-use categories according to relevant material parameters for the climate modelling; these data are presented in columns three to five of Table 2. For this study, all parameters have been calculated on a 20 m × 20 m grid.

To model the Olympic development (scenario B), updated input files are calculated based on information from Olympic Delivery Authority planning for the Olympic period (ODA 2008). The proposed development plans

land-use features for the site are drawn in a geographic information system programme as a series of polygons, such as roads, paths, building footprints and green spaces. Each polygon is then classified using the generalized land-use database classes (see Table 2). An estimated height value, based on descriptions within the planning documents, is associated with polygons classed as buildings. Figure 3 shows the model domain for the pre-Olympic and Olympic period scenarios in terms of the land-use categorizations.

The Olympic Legacy period (scenario C) inputs were derived from documents accessed via the London Development Agency (2008), which provided proposed land use and built from information for the Olympic development site. The GIS mapping was updated to include the new buildings, roads and paths for the Legacy period – note that the concourse area was reduced in size.

2.2.2. Morphology

Using the method developed by Evans (2009), the morphological site features for the model domain, including the Olympic development site, were estimated using polygons of the land-use feature taken from the Ordnance Survey's Ordnance Survey MasterMap (2010) dataset. The process involves using the height and footprint data to create extruded representations of the site features. These 3D features are then used to estimate the expected roughness features of the site, allowing an estimate of the spatial variation of the surface roughness parameter within the domain to be estimated. The site feature extrusions are also used to develop a 2D volume and height estimate or a NV (as defined in Hamilton et al. 2009). The NV is the total building volume normalized by the total footprint area. In this case, the NV is established for every grid point and is used to allocate the estimated anthropogenic heat emissions (described below).

2.2.3. Upwind meteorological data

The upwind heat flux data used to drive the *ADMS Temperature and Humidity* model were averaged from output

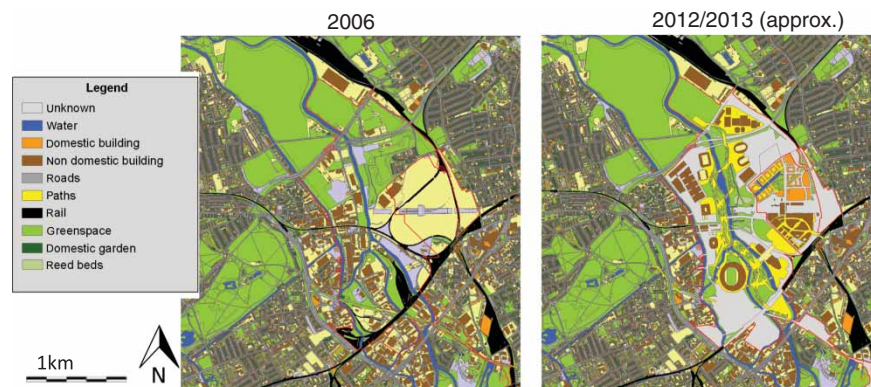


Figure 3. Olympic development site design and land use (2005 and 2012/2013).

of the LondUM, which outputs at 1 km² resolution; all of the ADMS models described above use a single, hourly varying meteorological condition to represent the upwind conditions entering the model domain.

The climate input used for the three periods is based on LondUM outputs for one-month spanning May/June period (1 km² grid) for the area around the Olympic development site for the base year of 2006. The base year is used for all three periods in order to ensure a consistent climate pattern

Table 3. Predicted annual heat emissions for Olympic development site.

Olympic development periods	Heat (MWh/yr)	Coolth (MWh/yr)	Electricity (MWh/yr)	Total (MWh/yr)
<i>Pre-Olympic period^a</i>				
Domestic	–	–	–	2030
Non-domestic	–	–	–	2020
Total	–	–	–	4050
<i>Olympic period^b</i>				
Main stadium	4310	1350	2240	7910
Aquatic	9420	–	2270	11,690
Velodrome	3540	720	1460	5720
Indoor arena	2050	410	850	3310
Eton Manor – tennis venue	370	70	150	590
Eton Manor – hockey venue	350	0	250	600
IBC/MPC ^c commercial	4090	1900	5690	11,680
IBC/MPC light industrial	3600	380	1770	5740
Multi-storey car park	0	0	650	650
Utilities	0	0	930	930
Athlete's village	18,320	0	11,480	29,800
Total	46,040	4840	27,740	78,620
<i>Olympic Legacy period^d</i>				
Venues	20,040	2560	7220	29,820
Multi-storey car park	0	0	650	650
Commercial	6130	2860	8540	17,530
Industrial	8970	940	4410	14,330
Utilities	0	0	930	930
Retail	270	450	1570	2280
Leisure	0	0	0	0
Community	420	0	110	530
School	1630	210	1030	2880
Residential	27,150	0	17,330	44,490
Total	64,610	7010	41,800	113,430

^aData derived from 'MSOA' energy statistics for London (DECC 2006).

^bData derived from 'OLY-GLB-ACC-DOC-ENG-01 Energy Statement' – Table 5 – Energy consumption and carbon-dioxide emissions from buildings within the Olympic Park.

^cInternational Broadcast Centre/Main Press Centre.

^dData derived from 'OLY-GLB-ACC-DOC-ENG-01 Energy Statement' – Table 11 – Indicative legacy energy use and emissions excl. Athlete's village and Stratford City.

and allow comparison between scenarios in the absence of weather variability. Weather files that take into consideration future climate scenarios, such as UKCIP09, were not used for the runs reported here as this would have added a further level of uncertainty to the model outputs.

2.2.4. Anthropogenic heat

The anthropogenic heat emissions are derived using the total annual, domestic, non-domestic, transport and metabolic anthropogenic energy (kWh) data for the development site using the technique set out in Hamilton et al. (2009) and Davies et al. (2008). This process resolves aggregate energy demands down to a local level. For buildings, the energy is allocated based on the NV – a value that describes the total volume over footprint area. This means that larger buildings receive a greater proportion of the aggregate energy demand. In smaller, homogenous areas, this is generally a suitable method of estimating the total annual energy demand where building specific estimates are unknown. This annual energy demand is then converted into an average annual heat emission (W/m²). Using the Olympic development site morphology and land-use input data, the grid points are filtered according to their classes and the anthropogenic energy is then apportioned to those points classed as 'Domestic Building' and 'Non-domestic Building' (i.e. class 2 and 3) for all points with a NV greater than zero, in proportion to the size of the value. In this work, we exclude emissions from transport and people.

The anthropogenic heat emissions (W/m²) for the three Olympic periods are modelled using total energy demand estimates drawn from Olympic Delivery Authority planning documents (ODA 2007). The total annual average heat emission for the venues and Olympic Athletes Village (see Table 3) is then associated with the relevant grid points that describe the venues, Village and legacy development; these values are then used in the modelling of the anthropogenic heat dispersion. These figures are indicative and highly dependent on the assumptions regarding the expected activities for the proposed building types and their expected energy efficiency. The values shown in Table 3 are converted into an annual average heat emission (W/m²) when associated with the relevant grid point.

3. Results

The land-use and anthropogenic heat models are used to calculate predictions of temperature variation on an hourly-basis, at either particular receptors, or on a regular output grid.

Figure 4 compares the average diurnal profiles for two locations within the modelling domain. The plot shows the average, minimum and maximum temperature perturbation diurnal profiles at two selected receptors: Stratford New Town (SNT) depot (black lines/circles) and the Hackney

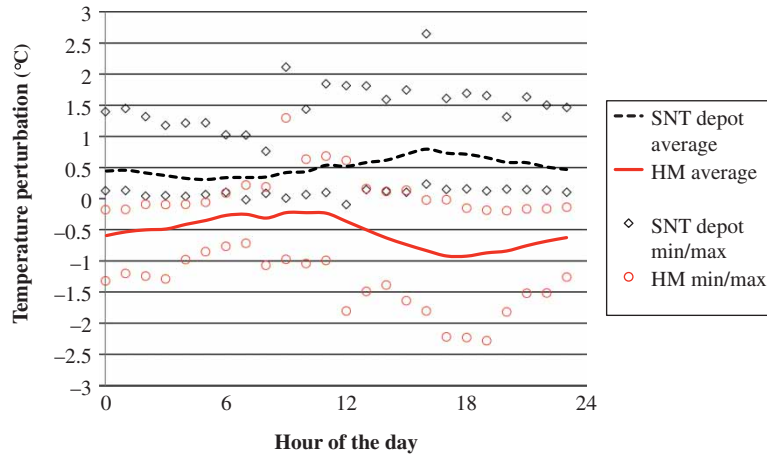


Figure 4. Modelled average diurnal profiles for HM and SNT depot.

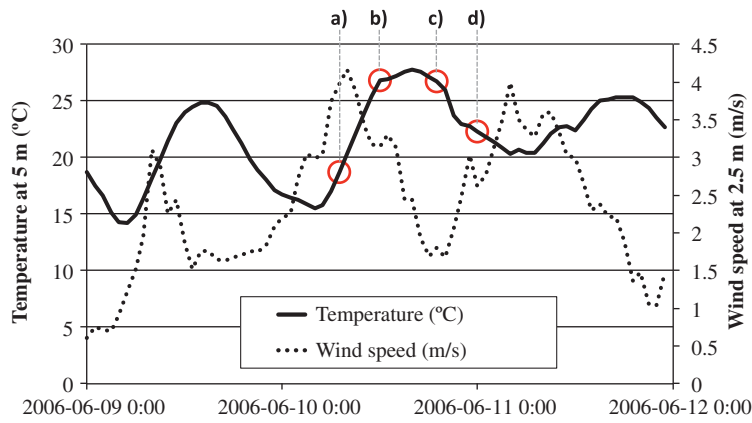


Figure 5. Measured upwind temperatures for development site.

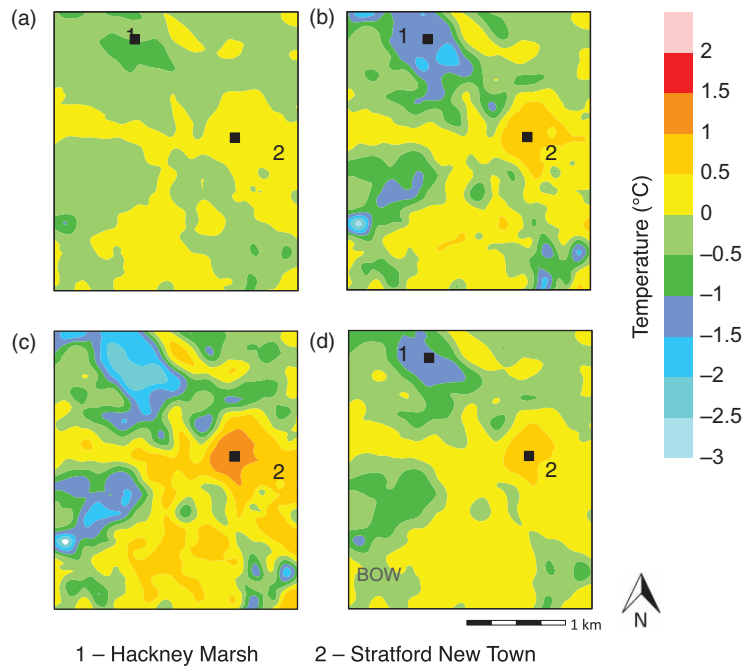


Figure 6. Modelled temperature perturbations to the upwind boundary-layer profile at 2 m due to land-use variations: (a) 07:00, (b) 12:00, (c) 19:00 and (d) 24:00 on 10 June 2006.

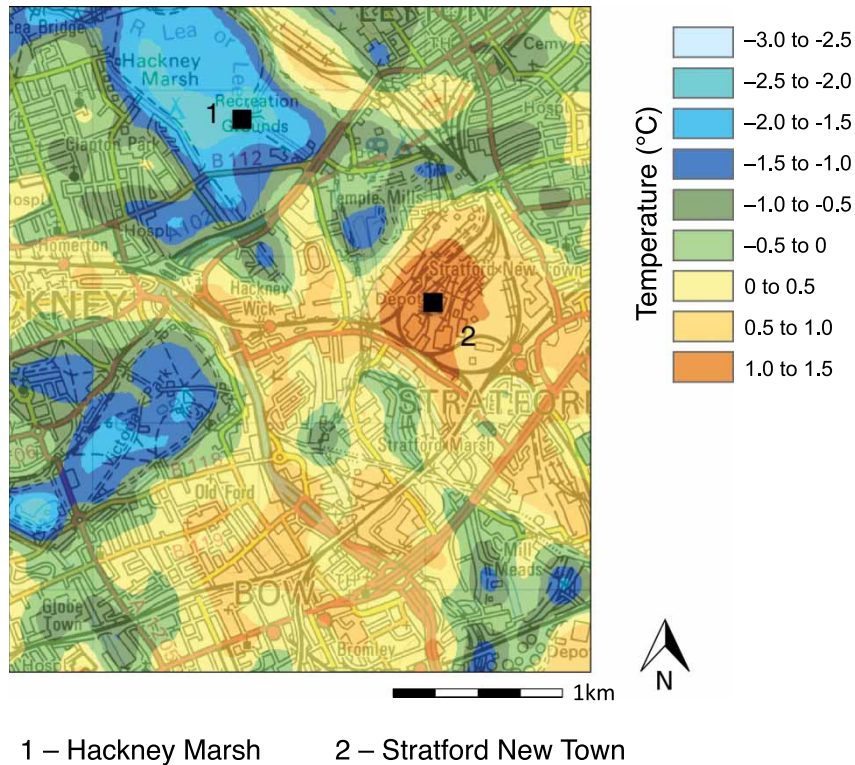


Figure 7. Modelled temperature perturbations to the upwind boundary-layer profile at 2 m due to land-use variations 19:00 on 10 June 2006 overlaid onto a map. ©Crown copyright, All rights reserved. 2009 Licence number 0100031673.

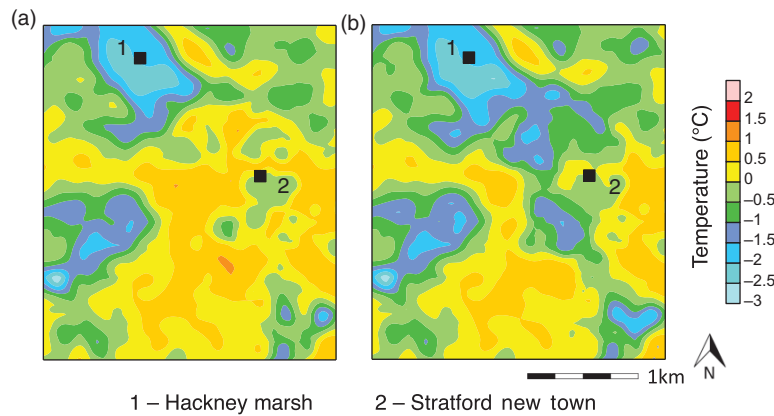


Figure 8. Modelled temperature perturbations to the upwind boundary-layer profile at 2 m due to land-use variations at 19:00: (a) 2012 and (b) 2030.

Marsh (HM) wetlands area (red lines/circles). The locations have been chosen to represent locations within the domain that achieve the extremes of the temperature variations, i.e. the SNT receptor is warmer than an average, and the HM receptor is cooler than average, although the receptors are only 1 km apart (refer to Figure 6 for locations). The model predicts that the maximum temperature perturbations occur during the hottest time of the day, i.e. during the afternoon. As a consequence, the maximum difference in temperatures between the two receptors, which is over one-and-a-half degrees, is greatest at this time.

Within the month period, three days were selected to be of particular interest due to relatively high temperatures. Figure 5 shows the upwind temperature (at 5 m) and wind speed (at 2.5 m) values for this period, which have been derived as a spatial average of the LondUM output. It can be seen that during this period, the diurnal temperatures are increasing, and the night time temperature on the third night does not drop below 20°C. The black circles indicate the times the gridded model output is presented, i.e. (a) 07:00, (b) 12:00, (c) 17:00, (d) 24:00 – referred to in Figure 6.

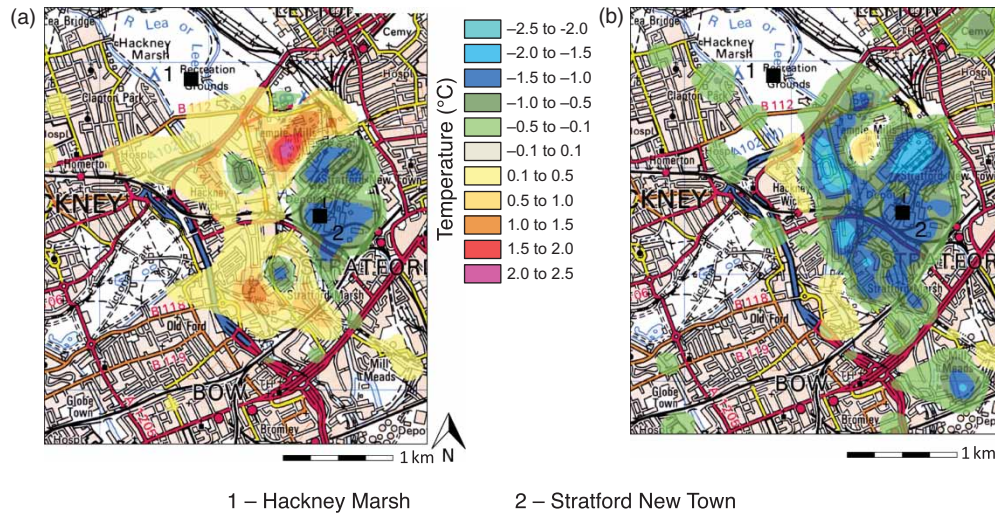


Figure 9. Difference plots of modelled temperature perturbations to the upwind boundary-layer profile at 2 m due to land-use variations at 19:00 between 2006 and (a) 2012 and (b) 2030. © Crown copyright, All rights reserved. 2009 Licence number 0100031673.

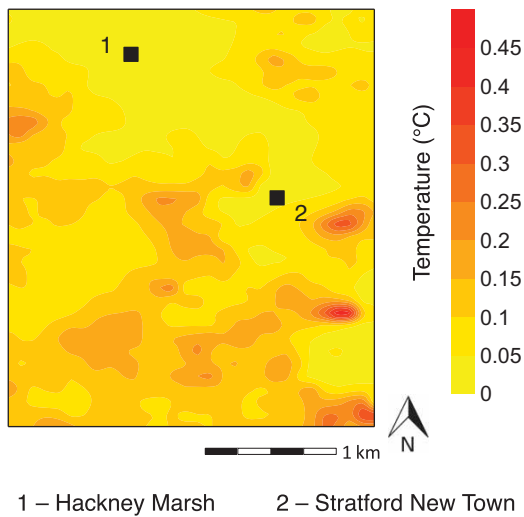


Figure 10. Modelled temperature increment to the upwind boundary-layer profile at 2 m due to anthropogenic heat from buildings at 19:00 (corresponding to Figure 7(c)).

3.1. Temperature for Olympic Parkland periods

Figure 6 shows contour plots of predicted temperature perturbations from the upwind profile at 2 m, for the hours indicated in Figure 5. In the early morning, the temperature is almost independent of the land use. At midday, there is a clear spatial pattern over the area, with the model predicting around a two-degree difference between the temperatures in the wetlands area compared to those in the SNT depot – locations which are just over a kilometre apart, but have significantly different physical properties. In the early evening around 19:00, the model predicts in excess of a 3°C difference in temperature between these two areas. This spatial variation decreases in magnitude over the course of the evening, to around a one-and-a-half degree difference by midnight.

Figure 7 shows the temperature perturbation at 19:00 overlaid onto a map. The temperatures predicted by the model are clearly related to the underlying land use, as would be expected. Note that the prevailing wind direction

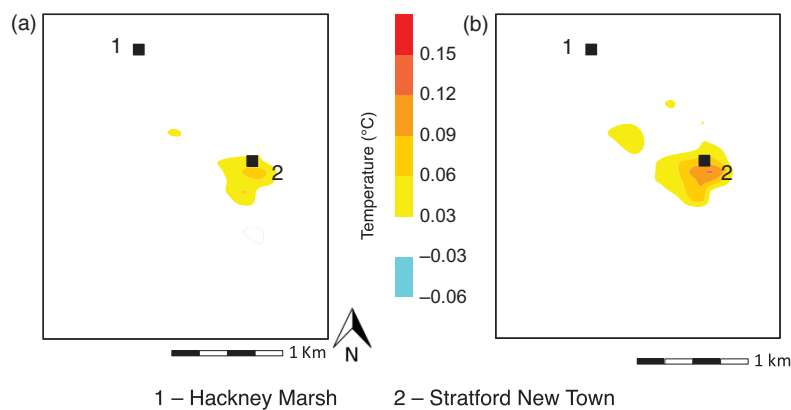


Figure 11. Difference plots of modelled temperature increments to the upwind boundary-layer profile at 2 m due to anthropogenic heat from buildings at 19:00 between 2006 and (a) 2012 and (b) 2030 (corresponding to Figure 9(a) and 9(b)).

for this hour was easterly and the advection of cool air can be seen to some extent in the north-western section of the study area.

Figure 8 shows the spatial variation of temperature predicted by the model at 19:00 for scenarios B and C, i.e. the plots corresponding to Figure 6(c). The change in land use in the SNT depot area has, in general, reduced the temperatures in this area, slightly in 2012, and significantly in the Legacy development, which includes an increase in the green area. In order to see the overall reduction in temperature relative to the pre-Olympic land usage, Figure 9(a) and 9(b) shows difference plots overlaid onto maps. The difference plots illustrate the effect of the concourse and 'back of house' features, which account for a significant proportion of the Olympic development area in the Olympic Period. The temperature differences here will be ultimately sensitive to the selected material parameters. The Olympic Legacy Site shows the influence of removing the hard surfaces (i.e. the concourse and 'back of house') despite the increased development density.

3.2. Anthropogenic heat

We also consider the change in anthropogenic heat due to new buildings on the Olympic site. Note that additional heat generated from the change in traffic behaviour is not included as part of this study.

Figure 10 shows a contour plot of the predicted temperature increment due to the anthropogenic heat from buildings in the model domain at 19:00 on 10 June 2006. The difference in scale of this plot compared to Figure 6(c) shows that, certainly for scenario A, the heat released from buildings is relatively small compared to the perturbations in temperature due to changes in land usage. Figure 11(a) and 11(b) shows difference plots for anthropogenic heat related to the pre-Olympic period, which correspond to those shown in Figure 9. The change in anthropogenic heat predicted by the model between the different scenarios is considered to be negligible.

4. Discussion

The results from the modelling of the London Olympic Parkland development illustrate how land-use and anthropogenic features can be taken into account in a local climate model and thus to assess the impact of a design proposal on local temperatures. In this paper we discussed the application a neighbourhood climate tool, i.e. *ADMS Temperature and Humidity* model, for modelling the temperature perturbation of three different design stages of the London Olympic Parkland site. Although the design and results are indicative, this paper illustrates how a tool of this type could be used to investigate the impact on local temperatures and the heat island in the design process. For example, during the Games or 2012/2013 period, it is shown that the addition of

the concourse, a relatively large impermeable surface feature of the site, has the effect of increasing local near-surface air temperature perturbations as compared to the baseline 2006 period. This is largely the result of the decreasing the surface albedo and increasing the area of high thermal admittance. These results are aligned with the analysis of weather and site parameters in Kolokotroni and Giridharan (2008). It is also shown that removing the concourse in the Legacy period and replacing it with permeable vegetated features reduces local temperatures as compared to the 2006 baseline. Note that although it is possible to quantify the impact of a development using this type of model, the results shown have a degree of uncertainty associated with the inputs and of the model formulation, and thus will represent a 'snapshot' or average of the land use, activities and weather experienced. Therefore, the results shown here are meant to reflect the magnitude and direction of perturbations that land-use changes associated with the London Olympic Parkland might have on local near-surface temperatures against a specified baseline.

Quantifying the relative impact that land-use and activity changes will have on local temperatures provides a basis to explore development designs at an early stage in the design process and presents an opportunity to potentially avoid otherwise unintended consequences associated with the design, as discussed in Hamilton, Davies, and Gauthier (2012). For example, not knowing or understanding how a development may change local temperature could result in discomfort during warm periods, which may have a detrimental impact on health and well-being, and may stress infrastructure and increase the demand for cooling. A strength of this integrated approach is that it can provide a direct quantitative, albeit relative, feedback to the designer of the impact that different design options may have on temperatures at different times of day and year, meaning that finding a design that can mitigate summer overheating and accrue winter benefits is more readily achievable. The use of this type of tool illustrates how an integrated design approach can offer benefits to designers and policymakers, in knowing what the likely impact will be and in particular for those areas that require UHI or climate change temperature mitigation.

5. Conclusions

This study presents a method of modelling perturbations to near-surface air temperature using the *ADMS Temperature and Humidity* model implementation, a neighbourhood-scale model that considers the impact of land use and morphology. The London Olympic Parkland site case study is used to illustrate the capabilities of such a model and the type of impacts that land-use changes can have, for a given set of designs and assumptions, on perturbing local neighbourhood-level temperatures. We modelled near-surface temperature perturbations from upwind values for a 16 km² domain encompassing the Olympic Parkland at

a 400 m² grid resolution for the pre-Olympic, Olympic, and Legacy periods to estimate the contribution the Parkland could have on local air temperatures.

The results of the modelling demonstrated how the development of the Olympic Parkland could influence local temperatures. These results are indicative but offer a useful assessment of the type and scale of temperature perturbations associated with changes in land use and anthropogenic heat emissions. The baseline model illustrates how the land-use features perturb the upwind temperature depending on the time of day, with a relative peak positive perturbation in temperature in the evening over the SNT development and a negative perturbation during the daytime over the HM. The potential impact of the 2012/2013 period development is to increase the local temperatures as compared to the 2006 baseline, which is attributed to the additional impermeable surfaces used for the concourse. The potential impact of the Legacy development is a negative perturbation of the upwind temperatures as compared to the 2006 baseline, which is attributed to the reduction of impermeable land cover and an increase green space. The relative impact of anthropogenic heat emissions on perturbing the upwind temperature is shown, in this case, to be small.

References

- Arnfield, A. J. 2003. "Two Decades of Urban Climate Research: A Review of Turbulence, Exchanges of Energy and Water, and the Urban Heat Island." *International Journal of Climatology* 23 (1): 1–26.
- Bohnenstengel, S. I., S. Evans, P. A. Clark, and S. E. Belcher. 2011. "Simulations of the London Urban Heat Island." *Quarterly Journal of the Royal Meteorological Society* 137 (659): 1625–1640. doi:10.1002/qj.855.
- Carruthers, D. J., R. J. Holroyd, J. C. R. Hunt, W.-S. Weng, A. G. Robins, D.D. Apsley, D.J. Thompson, and F.B. Smith. 1994. "UK-ADMS: A New Approach to Modelling Dispersion in the Earth's Atmospheric Boundary Layer." *Journal of Wind Engineering and Industrial Aerodynamics* 52: 139–153. doi:10.1016/0167-6105(94)90044-2.
- Carruthers, D. J., J. C. R. Hunt, and W.-S. Weng. 1988. "A Computational Model of Stratified Turbulent Airflow over Hills – FLOWSTAR I." In *Proceedings of Envirosoft. Computer Techniques in Environmental Studies*, edited by P. Zanetti, 481–492. Southampton: Springer-Verlag.
- Carruthers, D. J., and W. S. Weng. 1992. "The Effect of Changes in Surface Resistance on Temperature and Humidity Fields and Fluxes of Sensible and Latent Heat." *Boundary-Layer Meteorology* 60 (1–2): 185–199.
- CERC (Cambridge Environmental Research Consultants). 2010. *ADMS 4 – Temperature and Humidity: User Guide*. Cambridge: Cambridge Environmental Research Consultants, p. 50.
- CERC. 2011. *ADMS-Urban – An Urban Quality Management System: User Guide*. Cambridge: Cambridge Environmental Research Consultants, p. 334.
- CERC. 2012. "airText: Free Air Pollution, UV, Pollen and Temperature Forecasts for Greater London – Olympic Park." <http://www.airtext.info/temp>
- Davies, M., I. Hamilton, P. Steadman, A. Stone, I. Ridley, and S. Evans. 2008. "London's Anthropogenic Heat Emissions – Implications for Building Design." Proceedings of the World Renewable Energy Congress X and Exhibition, Glasgow, July 19–25.
- Environmental Protection Agency. 2009. "Urban Heat Island Basics." Accessed August 8, 2011. http://www.epa.gov/heat_island/index.htm
- Evans, S. 2009. "3D Cities and Numerical Weather Prediction Models: An Overview of the Methods Used in the LUCID Project." CASA Working Paper 148. University College London. Accessed June 5, 2011. <http://www.casa.ucl.ac.uk/publications/workingPaperDetail.asp?ID=148>
- Generalised Land Use Database. 2006. "Update." London: Department for Communities and Local Government. Product Code: 08FMD05741. ISBN: 978 1 4098 1119 0
- GLA (Greater London Authority). 2006. "London's Urban Heat Island: A Summary for Decision Makers." Accessed June 1, 2011. <http://legacy.london.gov.uk/gla/publications/environment.jsp>
- GLA. 2009. *The London Plan: Spatial Development Strategy for Greater London*. Consultation draft replacement plan. London: GLA.
- GLA. 2010. "The Climate Change Adaptation Strategy for London." Greater London Authority. Accessed September 9, 2011. <http://www.london.gov.uk/climatechange/>
- Grimmond, C. S. B., M. Blackett, J. Best, J. J. Baik, S. Belcher, S. I. Bohnenstengel, I. Calmet, et al. 2011. "Initial Results from Phase 2 of the International Urban Energy Balance Comparison Project." *International Journal of Climatology* 31 (2): 244–272.
- Grimmond, C. S. B., M. Blackett, M. Best, J. Barlow, J. J. Baik, S. Belcher, S. I. Bohnenstengel, et al. 2010. "The International Urban Energy Balance Models Comparison Project: First Results from Phase 1." *Journal of Applied Meteorology and Climatology* 49 (6): 1268–1292.
- Hamilton, I. G., M. Davies, and S. Gauthier. 2012. "London's Urban Heat Island: A Multi-scaled Assessment Framework." *Proceedings of the ICE – Urban Design and Planning* 1–12. doi:10.1680/udap.10.00046.
- Hamilton, I. G., M. Davies, P. Steadman, A. Stone, I. Ridley, and S. Evans. 2009. "The Significance of the Anthropogenic Heat Emissions of London's Buildings: A Comparison Against Captured Shortwave Solar Radiation." *Building and Environment* 44 (4): 807–817.
- Howard, L. 1818. *The Climate of London*. London: W. Phillips.
- Iamarino, M., S. Beevers, and C. S. B. Grimmond. 2012. "High-Resolution (Space, Time) Anthropogenic Heat Emissions: London 1970–2025." *International Journal of Climatology* 32 (11): 1754–1767. doi:10.1002/joc.2390.
- Ichinose, T., K. Shimodozono, and K. Hanaki. 1999. "Impact of Anthropogenic Heat on Urban Climate in Tokyo." *Atmospheric Environment* 33 (24–25): 3897–3909. doi:10.1016/S1352-2310(99)00132-6.
- Knowlton, K., C. Hogrefe, B. Lynn, C. Rosenzweig, J. Rosenthal, and P. Kinney. 2008. "Impacts of Heat and Ozone on Mortality Risk in the New York City Metropolitan Region under a Changing Climate." *Advances in Global Change Research* 30 (2): 143–160.
- Kolokotroni, M., and R. Giridharan. 2008. "Urban Heat Island Intensity in London: An Investigation of the Impact of Physical Characteristics on Changes in Outdoor Air Temperature During Summer." *Solar Energy* 82 (11): 986–998.
- London Development Agency. 2008. *People and Places – A Framework for Consultation*. London: London Development Agency.
- Mavrogiani, A., M. Davies, M. Batty, S. E. Belcher, S. I. Bohnenstengel, D. Carruthers, Z. Chalabi, et al. 2011. "The Comfort, Energy and Health Implications of London's Urban

- Heat Island." *Building Services Engineering Research and Technology* 32 (1): 35–52. doi:10.1177/0143624410394530.
- McMichael, A. J., P. Wilkinson, R. S. Kovats, S. Pattenden, S. Hajat, B. Armstrong, N. Vajanapoom, et al. 2008. "International Study of Temperature, Heat and Urban Mortality: The 'ISOTHURM' Project." *International Journal of Epidemiology* 37 (5): 1121–1131. doi:10.1093/ije/dyn086.
- ODA (Olympic Delivery Authority). 2007. *Olympic, Paralympic & Legacy Transformation Planning Applications – Energy Statement*. London: Olympic Delivery Authority.
- ODA. 2008. *Parklands and Public Realm Planning Submission: Design and Access Statement*. London: Olympic Delivery Authority.
- Offerle, B., C. S. B. Grimmond, and K. Fortuniak. 2005. "Heat Storage and Anthropogenic Heat Flux in Relation to the Energy Balance of a Central European City Centre." *International Journal of Climatology* 25 (10): 1405–1419. doi:10.1002/joc.1198.
- Office of National Statistics. 2005. *Neighbourhood Statistics. Generalised Land Use Database*. London: Office of National Statistics.
- Ojima, T. 1990. "Changing Tokyo Metropolitan Area and Its Heat Island Model." *Energy and Buildings*, 15 (1–2): 191–203.
- Oke, T. R. 1973. "City Size and the Urban Heat Island." *Atmospheric Environment* 7 (8): 769–779.
- Oke, T. R. 1987. *Boundary Layer Climates*. 2nd ed. London: Methuen.
- Oke, T. R. 1995. "The Heat Island Characteristics of the Urban Boundary Layer: Characteristics, Causes and Effects." In *Wind Climate in Cities*, edited by J. E. Cermak, A. G. Davenport, E. J. Plate and D. X. Viegas, 81–107. Netherlands: Kluwer Academic.
- Ordnance Survey Mastermap. 2010. © Crown Copyright/Database Right 2010. An Ordnance Survey/EDINA Supplied Service.
- Porson, A., I. Harman, S. Bohnenstengel, and S. Belcher. 2009. "How Many Facets Are Needed to Represent the Surface Energy Balance of an Urban Area?" *Boundary-Layer Meteorology* 132 (1): 107–128. doi:10.1007/s10546-009-9392-4.
- Raupach, M. R., W. S. Weng, D. J. Carruther, and J. C. R. Hunt. 1992. "Temperature and Humidity Fields and Fluxes Over Low Hills." *Quarterly Journal of the Royal Meteorological Society* 118 (504): 191–225. doi:10.1002/qj.49711850403.
- Sailor, D. J. 2010. "A Review of Methods for Estimating Anthropogenic Heat and Moisture Emissions in the Urban Environment." *International Journal of Climatology* 31 (2): 189–199.
- Stocker, J. R., G. Virk, D. J. Carruthers, S. I. Bohnenstengel, I. G. Hamilton, S. Evans, and M. Davies. Forthcoming. "Modelling Local Perturbations To Temperature and Humidity in an Urban Environment."
- Stull, R. B. 1988. *An Introduction to Boundary Layer Meteorology*. 1st ed. Netherlands: Kluwer Academic Publishers, p. 667.
- Taha, H. 1997. "Urban Climates and Heat Islands: Albedo, Evapotranspiration, and Anthropogenic Heat." *Energy and Buildings* 25 (2): 99–103.
- Thomson, D. J. 2000. "ADMS Met Input Module." UK Met Office. http://www.cerc.co.uk/environmental-software/assets/data/doc_techspec/CERC_ADMS4_P05_01.pdf
- Watkins, R., J. Palmer, M. Kolokotroni, and P. Littlefair. 2002. "The London Heat Island: Results from Summertime Monitoring." *Building Service Engineering* 23 (2): 97–106. doi:10.1191/0143624402bt0310a.
- White, A., and M. Holmes. 2009. "Advanced Simulation Applications Using ROOM." Proceedings of the eleventh conference of IBPSA, Glasgow, July 27–30.

Appendix. ADMS Temperature and Humidity sensitivity studies

Extensive sensitivity tests were performed during the development of the *ADMS Temperature and Humidity* model. Each of the five parameters that define the land use and morphology were varied within physically realistic ranges; the parameter space of values used for the investigations are given in Table A1. The model set-up has a domain of size of 36 km² in which all parameters were kept constant, with the exception of an inner square region of size approximately 1 km², in which the parameter values were varied. The perturbations to the upwind profile of temperature and humidity predicted by the model were inspected in details to ensure that the model behaves as expected. For these investigations, the upwind meteorological conditions are output from LondUM for a three-day period in June 2008.

The model results for some particular cases are given in Figure A1. The average diurnal variation of temperature over the three-day period is presented for a location towards the downwind edge of the inner region. The temperature perturbation output from the model is 'at 2 m', recalling that the model does explicitly model the three-dimensional features of the urban landscape. The parameters defined in the outer region are taken to represent an 'urban base case' (given in bold in Table A1). For each of the test cases, one parameter is altered within the inner region.

The model output is discussed below:

Test 1. Increasing albedo

The value of albedo used in the inner region is 0.4, compared to the value of 0.1 used in the outer region. This change in albedo could represent an area where the buildings had been constructed of materials with a higher than usual reflectivity, or alternatively, the buildings could be painted with a light colour. The inner region reflects more of the short-wave radiation compared to the outer region, and as a consequence the temperature is lower. This phenomenon only occurs during daylight hours, and the minimum in temperature predicted by the model corresponds to the time at which the incoming solar radiation is highest, i.e. at midday.

Test 2. Decreasing building density

The building density for the 'urban base case' was selected as a case where the buildings were reasonably close together, such as occurs in some southern European cities. Decreasing the building density (taking a NV of 2.5 m) allows more incoming short-wave radiation to be trapped between the buildings, which leads to an increase in temperature close to the ground. This phenomenon only occurs during daylight

Table A1. Summary of sensitivity tests performed with the *ADMS Temperature and Humidity* model.

Range	Albedo (–)	Thermal admittance (J/(K m ² s ^{1/2}))	Surface resistance to evaporation parameter (s/m)	Surface roughness (m)	NV (m)
Lower	0	500	0	0.001	0
	0.1	1000	50	0.01	2.5
Mid	0.2	1500	100	0.1	5
	0.3	2000	200	1	10
Upper	0.4	2500	300	2	20

Note: Parameters in bold indicate those used to represent the 'urban base case' for outer domain in the sensitivity testing.

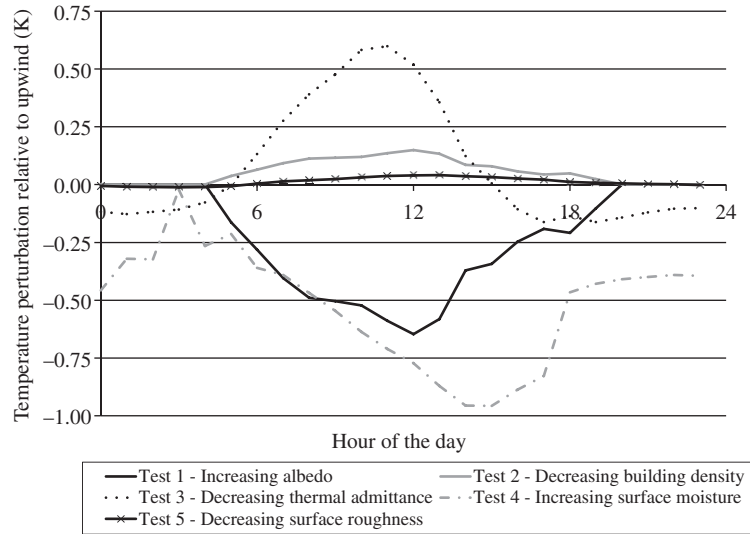


Figure A1. Sensitivity test results: average diurnal temperature perturbations for a three-day period in June 2008. Values shown are for a point in the inner domain, close to the downwind edge.

hours, and the maximum in temperature predicted by the model corresponds to the time at which the incoming solar radiation is highest, i.e. at midday. It should be noted that the model does not account for the changes in long-wave radiation relating to building density variations.

Test 3. Decreasing thermal admittance

The thermal admittance of the inner domain was selected to approximately represent that of a parkland area, that is $500 \text{ J}/(\text{K m}^2 \text{ s}^{1/2})$. This lower thermal admittance leads to increased temperatures during the day relative to the outer domain, as less heat can be stored in the ground. Conversely, in the late afternoon and during the night, the temperature in the inner domain is reduced, as there is less heat available for re-release.

Test 4. Increasing surface moisture

The inner domain is taken to have an increased amount of moisture compared to the outer domain, for instance, a parkland area with paths and some buildings (surface resistance to evaporation value of 100 s/m). There is a decrease

in temperature in the inner domain throughout the day and night, with the minimum local temperature perturbation corresponding to the time at which the ambient temperature achieves a maximum value.

Test 5. Decreasing surface roughness

The roughness in the inner domain is decreased to 0.1 m , a value that in reality is too low to be representative of any land use within an urban area, and as such this test should be considered to be for demonstration purposes only. The decrease in roughness causes a slight increase in the temperature during the daytime, as the temperature profile has an increased gradient in the low roughness area. As the gradient of the temperature profile is inverted at night, the consequence of the region of decreased roughness is a very slight decrease in temperature at that time.

The selection of tests discussed above demonstrates that the *ADMS Temperature and Humidity* model performs as expected with respect to the sign of the temperature perturbation predicted for bulk changes in input parameters.